Society For Biomaterials

In vitro evaluation of human endometrial stem cell-derived osteoblast-like cells' behavior on gelatin/collagen/bioglass nanofibers' scaffolds

Esmaeel Sharifi,[1,2] Somayeh Ebrahimi-Barough,[2] Maryam Panahi,[3] Mahmoud Azami,[2] Arman Ai,[3] Zahra Barabadi,[2] Abdol-Mohammad Kajbafzadeh,[2,4] Jafar Ai[2,5]

[1]Cellular and Molecular Research Center, Shahrekord University of Medical Sciences, Shahrekord, Iran
[2]Department of Tissue Engineering and Applied Cell Sciences, School of Advanced Technologies in Medicine, Tehran University of Medical Sciences, Tehran, Iran
[3]School of Medicine, Tehran University of Medical Sciences, Tehran, Iran
[4]Pediatric Urology Research Center, Section of Tissue Engineering and Stem Cells Therapy, Department of Pediatric Urology, Children's Hospital Medical Center, Tehran, Iran (IRI)
[5]Brain and Spinal Injury Research Center (BASIR), Imam Khomeini Hospital, Tehran University of Medical Sciences, Tehran, Iran

Received 10 September 2015; revised 28 March 2016; accepted 15 April 2016
Published online 5 May 2016 in Wiley Online Library (wileyonlinelibrary.com). DOI: 10.1002/jbm.a.35748

Abstract: New biomimetic nanocomposite scaffold was prepared by the combination of nanofibrilar bioglass containing copper ion as the inorganic phase and gelatin/collagen as the organic phase of bone tissue. In this study for fabrication of the scaffold, freeze drying and electrospinning methods were used, and genipin was used as the cross-linking agent for increasing the mechanical properties of the scaffold. The growth and viability of human endometrial stem cell-derived osteoblast-like cells were investigated on this biomimetic scaffold. Cellular biocompatibility assays illustrated that this scaffold has more viabilities and osteoblast growths in comparison with two-dimensional culture. Copper ion increased growth of the osteoblasts on nanocomposite scaffold containing nanofibrous bioglass. Thus, the results obtained from this study indicate that the prepared scaffold is suitable for osteoblast growth and attachment; thus, potentially, this nanocomposite scaffold is an appropriate scaffold for bone tissue engineering. © 2016 Wiley Periodicals, Inc. J Biomed Mater Res Part A: 104A: 2210–2219, 2016.

Key Words: biomimetic, nanofibrilar bioglass, nanocomposite, endometrial stem cells, osteoblast cells

How to cite this article: Sharifi E, Ebrahimi-Barough S, Panahi M, Azami M, Ai A, Barabadi Z, Kajbafzadeh A-M, Ai J. 2016. *In vitro* evaluation of human endometrial stem cell-derived osteoblast-like cells' behavior on gelatin/collagen/bioglass nanofibers' scaffolds. J Biomed Mater Res Part A 2016:104A:2210–2219.

INTRODUCTION

Bone tissue engineering is a promising technology for regenerating defected and diseased bone tissue. Nowadays, by tissue engineering, utilizing cells, and three-dimensional biodegradable scaffolds,[1] bone tissue defects can be regenerated. Tissue engineering is mainly based on seeding cells on porous biodegradable three-dimensional scaffolds to construct three-dimensional tissue structures.[2] A suitable scaffold should have special properties, such as porosity, appropriate pore morphology/size, appropriate chemical, physical, and well mechanical properties.[2,3] Thus, as a primary function, the scaffold is a bed for cell adhesion, proliferation, growth and differentiation, and organizing the bone cells into a healthy new bone as the scaffold degrades. In this regard, design and manufacturing of suitable scaffolds and using the cells are of particular importance. Main challenge in designing tissue engineering scaffolds is the fact that many materials are not simultaneously resistant and bioresorbable; mechanically, resistance/strong substances are usually bioinert, while biodegradable and bioactive biomaterials have a tendency to be mechanically weak.[2] Thus, composite scaffolds made of biodegradable polymers and bioglasses can provide suitable structures containing bioactivity, biodegradability, and mechanical resistance.[3] Many porous nanocomposite scaffolds have been studied and fabricated using various methods, such as foam casting, solvent leaching, freeze drying, foamy procedure, and electrospinning.[4] These scaffolds allow cells to fabricate three-dimensional tissue structures through cell adhesion and proliferation, generating extracellular matrix (ECM).[5,6] Recent advances in biomaterial science have provided various substances that are desirable substitutes for bone tissue defects.[7,8] The most important substances in this

Correspondence to: J. Ai; e-mail: jafar_ai@tums.ac.ir
Contract grant sponsor: Tehran University of Medical Sciences and Iranian National Science Foundation; contract grant number: 91042417

group of biomaterials are calcium phosphates and bioglasses that have clinical usage nowadays.[7–10] Due to possessing high biocompatibility and the ability to produce mineral phase similar to bone tissue, bioglasses have many applications in bone tissue engineering, particularly in orthopaedic, maxillofacial surgery, and dentistry.[9,11]

In addition, setting of the mineral phase beside the collagen base in the natural bone structure can provide us with new ideas to mimic the bone tissue structure.[12–14] Polymer-ceramic composites used in bone tissue engineering are nanofibers filled with nanoparticles showing a type of nanocomposite system, which are well known for the accelerated mechanical strength and biofunctionality.[5,15,16] Scaffolds containing nanoparticle structures, such as hydroxyapatite and beta-tricalcium phosphate, possess compatibility to the bone tissue, while adding carbon nanofiber induces mechanical strength and electrical conductance in the scaffold.[17]

Scaffolds used for this purpose should mimic ECM structure and function.[5,17] Electrospinning is a diverse method for constructing biodegradable scaffolds containing fibers with the size similar to ECM fibrils.[18,19] Electrospinning can produce nanofibrilar scaffolds from natural or synthetic polymers[5,15] and also from polymer-ceramic composites (particularly in bone tissue engineering).[3,18] An effective aspect of bone tissue engineering is the use of functional segregated cells and biodegradable scaffolds provided by engineered biological materials.[14,19] At present, bioactive glasses and related composite materials are known as the best scaffold substances for bone tissue engineering.[17,19] Bioactive glasses are subsets of bioactive minerals that are able to interact with physiological fluids to produce connection with bone for generating hydroxyapatite layers similar to the bone.[12,20] It has been demonstrated that bioglass surface interactions induce the release of P, Ca, Si, and Na ions,[21] which subsequently induce appropriate intracellular and extracellular responses, resulting in the rapid regeneration of bone tissue.[22]

One of the most common scaffolds used in bone tissue engineering is 45S5 bioglass.[23] The main characteristic of this bioglass is releasing ions, such as Ca, Si, P, and Na, which can induce proper cellular interactions, resulting in an accelerated bone tissue formation.[24–26] Moreover, in tissue engineering and cell therapy, various stem cells have been used for the treatment of different diseases.[27,28] Previous studies have shown that mesenchymal stem cells (MSCs), hematopoietic stem cells, and embryonic stem cells can differentiate into osteoblast cells.[29,30] Human endometrial stem cells (hEnSCs), as a new source of MSCs, are responsible for reformation and remodeling of human endometrium in the menstrual cycles.[31–33] It has been shown that hEnSCs can differentiate into various cells, and these cells could be considered for tissue engineering and cell therapy due to its dynamic nature.[34,35] In this study, we aim to fabricate nanofibrilar 45S5 bioglass by electrospining method and then constructing a suitable scaffold through a freeze-drying process for bone tissue engineering by adding the nanofibrilar bioglass to hydrogel. Then, cell viability and activity of differentiated osteoblast cells derived from endometrial stem cells (hEnSCs) on fabricated scaffolds are evaluated.

MATERIALS AND METHODS

Preparation and isolation of endometrial stem cells

hEnSCs, were isolated according to our previous study.[36] In brief, the biopsy samples were washed in Dulbecco's phosphate-buffered saline and then treated with collagenase I (1 mg/mL; Gibco) for 60 minutes at 37°C. The digested cells were passed through 40 and 70 μm sieves. After centrifuging the cells, Ficoll purification was applied. Isolated cells were cultured in Dulbecco's modified Eagle medium (DMEM)/F12 medium containing 1% antibiotic penicillin/streptomycin, 10% fetal bovine serum (FBS), and 1% glutamine, followed by incubation at 37°C with 5% CO_2. The media were changed every 3 days. The hEnSCs at passage 3 were used for experiments.

Differentiation of hEnSCs into osteoblast-like cells

The hEnSCs were seeded in 24-well tissue culture, at the concentration of 2×10^4 cells/mL with 0.5 mL completed DMEM per well. After 24 hours, osteogenic media containing $10^{-7}M$ dexamethasone + 50 g/mL L-ascorbicacid-2-phosphate and 10 m*M* beta-glycerolphosphate were added to cultured cells. The hEnSCs were cultured in this osteogenic condition for 21 days at 37°C in 5.5% CO_2. The medium was changed every 3 days. After 21 days, alizarin red (Sigma) staining was performed. Alizarin red method was used to verify the calcification and mineralization of ECM. In this procedure, on day 21, the cultured cells were fixed in 4% paraformaldehyde (Sigma) for 30 minutes, followed by staining with 2% alizarin red at ambient temperature. Phase contrast microscope was used for the evaluation of alizarin red-stained area.

Fabrication of nanocomposite scaffold

Fabrication of nanofibrilar bioglass. The copper containing 45S5 (45 wt % SiO_2, 6 wt % P_2O_5, 23.5 wt % CaO, 1 wt % CuO, and 24.5 wt % Na_2O) bioglass nanofibers are composed of tetraethyl orthosilicate (TEOS) ($Si(OC_4H_9)_4$, 99.99%; Sigma-Aldrich), triethyl phosphite ($P(OEt)_3$, $P(C_2H_5O)_3$, 99.5%; Sigma-Aldrich), calcium nitrate tetrahydrate ($Ca(NO_3)_2{\cdot}4H_2O$, 99.60%; Sigma-Aldrich), and sodium nitrate ($NaNO_3$, 100.40%; Sigma-Aldrich). Gel-derived copper containing 45S5 bioglass was prepared as follows: initially 33.5 mL TEOS was added to 1*M* nitric acid, with H_2O:TEOS molar ratio equal to 18; to prepare the required amount of 1*M* nitric acid solution, 3.26 mL of 69% nitric acid was mixed with 47.6 mL of distilled water. The solution was allowed to react for 60 minutes for hydrolysis of the precursor through stirring. The following reagents were added separately after 45 minutes during stirring, in the following sequence: 2.9 mL triethyl phosphate, 19.84 g calcium nitrate tetrahydrate, 13.52 g sodium nitrate, and 0.61 g copper(II) nitrate trihydrate.[37,38] The sol mixtures were stirred for 36 hours and aged without stirring at 25°C for 24 hours, followed by further 24 hours at 40°C. Prior to electrospinning, the 12 wt % solution of PVA was prepared and mixed

with sol–solution in ratio of 1:1.5, then 5 mL of this solution was loaded in syringe and under controlled condition (voltage: 20 kV, distance: 10 cm, and injection rate: 1 mL/h), and electrospinning process was done. The nanofibers were subsequently heat treated at 700°C for an hour in air with a heating rate of 4°C/min and a cooling rate of 5°C/min. The heat treatment temperature was determined to be high enough to eliminate organic sources and nitrates completely.[38]

Fabrication of nanocomposite hydrogel. Porous gelatin/collagen/nanofibrilar bioglass (copper containing 45S5 bioglass) nanocomposites were fabricated as follows: At first, collagen/gelatin solution with the ratio of 1:9 (Merck, microbiology grade, catalogue number 104070) was prepared. For this purpose, collagen was added to deionized water containing 50 m*M* acetic acid, and gelatin was added to deionized water in a stirrer associated with heating. After 1 hour, collagen and gelatin solutions were mixed to make a 10% (w/v) solution. In the case of GEL/Col/nanofibrilar copper containing 45S5 bioglass nanocomposites, the ratio of organic–inorganic was 70%:30%.[12] In the next step, the fiber was mixed with hydrogel through gentle vortex. Then the prepared hydrogel and the nanocomposite hydrogel were poured into a cylindrical mold and kept at 4°C for 2 hours until physical gelation occurred. Afterward, the gel was extracted and kept at −20°C for about 24 hours. The resultant nanocomposite was extracted and freeze dried to create a porous structure. Scaffolds were incubated in a 0.5% genipin solution for 16 hours. Samples were washed with ethanol, PBS, and deionized water to remove remnants of the genipin. The provided scaffolds were kept at a dry place.

Characterization of scaffold

Scanning electron microscopy. Scanning electron microscopy (SEM; Philips XL30 microscope) was used to evaluate the morphology of nanofibers and porous structure of nanocomposite scaffold. Before SEM investigation, the surface of all samples was coated with gold by the mean of gold-sputtering device. Then by using 15 kV accelerating voltage, photographs were taken from the nanocomposite scaffold and nanofibers.

Differential scanning calorimetry and thermogravimetric analysis. For determination of mass loss and transition temperature of nanofibrilar bioglass, differential scanning calorimetry and thermogravimetric analysis (DSC–TGA) was performed. The sol–gel-derived nanofibrilar bioglass, produced by electrospinning, was used in this analysis. Transformations including their temperatures and sample weight loss from room temperature up to 1000°C were assessed, and the heating rate of apparatus was 5°C/min.

Mercury porosimetery. Mercury porosimeter (PASCAL140, Germany) was applied for measuring the porosity percentage, mean value of pores' diameter, and the distribution of nanocomposite scaffold pores. For these reasons, nanocomposite scaffold was dried initially, and then at high vacuum, mercury was exposed to the samples. The pressure of mercury was changed from 0.1 to 400 kPa incrementally, which can show pore size ranging from 3 nm to 200 μm. Subsequently, mercury penetrated through pores; at low pressures, big pores were filled with mercury, and at higher pressures, mercury infiltrated through smaller pores. The pore diameter was determined by Washburn equation ($L = \gamma Dt/4\eta$). L is the infiltrated mercury volume, γ is the surface tension, D is the diameter of pores, T is the time of mercury infiltration through pores, and μ is the mercury viscosity. By this method, size of the pores can be determined through the range of 350–100,000 Å.

Structural analysis

Fourier transform infrared spectroscopy. Bomem MB 100 spectrometer was used for investigating the functional groups of nanocomposite scaffold. For this, 1 mg of the powder nanocomposite scaffold was carefully mixed with 300 mg of KBr (at infrared grade) and then pelletized under vacuum. Fourier transform infrared spectroscopy (FTIR) analysis of pellets was performed in the wavelength range of 400–4000/cm at a scan speed of 23 scan/min with 4/cm resolution.

X-ray diffraction. After heating at 700°C, the nanofibrilar bioglass was analyzed by X-ray diffraction (XRD) on a Philips X-ray diffractometer with Co-K_α radiation ($\lambda = 1.78901$ Å). Crystallographic properties of nanofibrilar bioglass were obtained using XRD method. XRD diagram was recorded in step mode (measurement time 1 s, step size 0.02°, measurement temperature 25°C, and standard: Si powder). The scans of the selected diffraction peaks were carried out in crystallographic identification of the phases of synthesized nanofibers, which was accomplished by comparing experimental XRD patterns with standards compiled by the International Center for Diffraction Data.

Cell seeding on the prepared scaffolds and cells' attachment analysis by SEM. hEnSC-derived osteoblast-like cells were cultured in DMEM/F12 (Gibco) supplemented with 10% FBS, 50 U/mL penicillin, and 50 U/mL streptomycin at 37°C with 5% CO_2, and the medium was changed every 2 days and then was digested with 0.25% trypsin for 5 minutes to create a single cell suspension. Following trypsinization, the scaffolds were cut into small pieces of 15 mm in diameter and sterilized with ultraviolet light overnight. Then cells were plated on the prepared scaffold with 3×10^5 cells per scaffold in 24-well plates and incubated in DMEM/F12 at 37°C for 4 hours to allow hEnSCs to diffuse into and adhere to the scaffold before the addition of culture medium to each plate. Then humidified atmosphere containing 5% CO_2 was used to the incubation of scaffold constructs containing the cells for 4 days at 37°C. Then, PBS was used for washing the samples twice before fixation procedure. The fixation was carried out as follows: samples were immersed in 2.5% glutaraldehyde for 1 hour. Dehydration was done by a series of graded acetone

TABLE I. Primers Used for Real-Time RT-PCR

Gene	Accession Number	Length (bp)	Primer Sequence (5′–3′)	Annealing (°C)
SPP1	NM_000582	21	F TCACCTGTGCCATACCAGTTA	57
		20	R GGCCACAGCATCTGGGTATT	
ALPL	NM_000478	19	F CTATCCTGGCTCCGTGCTC	57
		20	R ACTGATGTTCCAATCCTGCG	
SPARC	NM_003118	21	F CTGCAGAAGAGATGGTGGCGG	57
		21	R CAGGCAGGGGGCAATGTATTTG	
GAPDH	NM:002046.3	15	F TCGCCAGCCGAGCCA	57
		20	R CCTTGACGGTGCCATGGAAT	

solutions. At last, samples were kept in a hood for air drying and then used for SEM investigation.

Cell viability and proliferation assay. The 3-(4,5-dimethylthiazoyl-2-yl)-2,5-diphenyltetrazolium bromide (MTT) reduction assay was used for metabolic activity of the hEnSC-derived osteoblast-like cells cultured on the scaffolds at 1, 2, and 4 days after cell seeding. The cells were seeded at a density of 3×10^5 cells/scaffold in 24-well plates and incubated under standard condition for 1, 2, and 4 days. For this test, MTT powder (Sigma, Germany) was dissolved in warm PBS (37°C)[28] to prepare 5 mg/mL MTT solution. Then, 40 μL of 5 mg/mL MTT solution was added to each well, and the plates were incubated at 37°C for 4 hours. The medium was removed, and the formazan crystals were dissolved in dimethylsulfoxide 99.5% (Sigma, Germany), and the plate was shaken for 5 minutes with a shaker. The formazan solution transferred to 96-well plate, and absorbance at 570 nm was measured using a microplate reader (Expert 96; Asys Hitch, Ec Austria).

Quantitative reverse transcription-polymerase chain reaction

Detection and comparison of gene expression of osteopontin (218 bp), alkaline phosphatase (ALP; 568 bp), and osteonectin (248 bp) were performed with quantitative reverse transcription-polymerase chain reaction (qRT-PCR) between two-dimensional and three-dimensional groups. qRT-PCR was done after 21 days induction of endometrial stem cells with osteogenic media in tissue culture plate (two-dimensional group) and scaffold (three-dimensional group). Primer sequences designed for this reaction are listed in Table I. Total RNA was extracted using the RNeasy Plus Mini kit (Qiagen) according to the manufacturer's protocol. DNaseI, RNase-free kit (Takara, Shiga, Japan), was used for removing genomic DNA of osteoblast cells. Revert Aid First Strand cDNA Synthesis kit (Takara) was used for synthesizing the complementary DNA. Relative gene expression analysis was performed with real-time PCR. In each PCR, 1× Power SYBRH Green PCR Master Mix (ABI PRISM, 4368702) was mixed with 12 ng cDNA and specific primers in a total volume of 20 μL. Thermal conditions were used for all genes noticed in Table I. The comparative Ct method, $2^{-\Delta\Delta Ct}$, was used for relative gene expression analysis. All Ct values calculated from the target genes were normalized to GAPDH and calibrated using calculation from the undifferentiated hEnSCs. In each experiment, there were at least three independent experiments, and these were done in duplicates.

ALP production activity evaluation

Density of 3×10^5 cells/cm^2 was seeded in each well (of 24-well culture plate) containing nanocomposite scaffolds in each well. One well of each plate without any composite sample was used as a negative control group (TPS). At days 1 and 7 after cell seeding, ALP activity was evaluated. At the end of these times, culture media were decanted, cells cultured on scaffolds were washed with PBS and homogenized by sonication in lysis buffer containing 500 μL deionized water plus 25 μL 1% Triton X-100. After these steps, the total protein content of cells was determined using a commercially available kit (Micro/Macro BCA; Pierce Chemical, Rockford, IL). In addition, ALP activity was measured by commercial kinetic kit (Pars Azmun, Iran) based on the conversion of *p*-nitrophenyl-phosphate to *p*-nitrophenol and phosphate at 37°C and pH = 9.8. The absorbance change was monitored by using spectrophotometrically at 405 nm at 37°C temperature. ALP levels were normalized to the total protein content of cells at the end of the experiment. All tests were repeated three times ($n = 3$), and SPSS software was used for statistical analysis. Student's *t*-test was used to determine significant differences between the groups. p value <0.05 was considered as statistically significant.

Statistical analysis

The data are presented as mean ± standard deviation of the mean ($n = 3$). A one-way analysis of variance was used to compare the mean of different data sets, and the value of $p < 0.05$ was considered as statistically significant.

RESULTS

Characterization of isolated hEnSCs

hEnSCs are adherent cells, and their adherence to the cell culture flask makes this property useful for their isolation. After three passages, homogeneous hEnSCs with spindle or elongated shapes appear [Figure 1(a)] in the culture flask. According to our previous published report,[36] flow cytometric results showed that immunophenotyping was negative for CD31, CD133, and CD34 and positive for OCT4, CD44, CD90, and CD105. After 21 days, cells cultured in osteogenic media were stained with alizarin red [Figure 1(b)]. Calcium nodule formation and calcium deposition can be seen dark red in the picture.

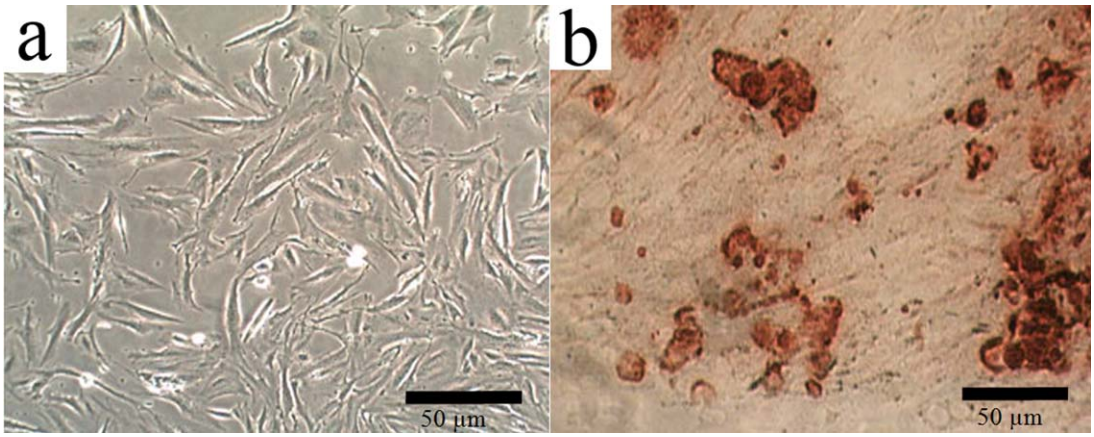

FIGURE 1. a. Morphology of EnSCs, b. Alizarin red staining.

Differential scanning calorimetry and thermogravimetric analysis

To get the right heating temperature of bioglass nanofibers, DSC–TGA was performed. As shown in Figure 2, DSC–TGA curves get from sol–gel derived nanofibrilar bioglass between room temperature and 1000°C. In DSC curves, endothermic and exothermic peaks are observable. At 75°C, the first endothermic peak started, and this peak corresponds to the release of physically adsorbed water on the surface of nanofibers; as TGA trace demonstrated between 75 and 160°C, all water and products from the polycondensation reaction were removed (12% weight loss). At 350°C, the other two endothermic peaks started, which related to the release of water from the further condensation of P–OH and silanol group, pyrolysis reaction of free organic species, burning of PVA, and the removal of nitrates, which are usually removed in the thermal stabilization process (41% weight loss). Total nitrate species was removed at 560°C (22% weight loss). It was mentioned that two observed peaks at 350 and 582°C may correspond to the burning of nitrate/PVA and decomposition of hydrocarbon molecules, respectively, in that temperature.

Endothermic peaks correspond to the removal of sodium nitrite and other nitrogen compounds. On the other hand, the exothermic peak indicates the formation of a crystalline phase and phase transformation. The best stabilization temperature, with high bioactivity and removal of all nitrogen contents, is about 700°C according to a previous study.[38] As shown in this figure, no significant weight loss was observed above 700°C. This curve confirmed that removal of the residuals was before 700°C, so this temperature is suitable for the stabilization of nanofibrilar bioglass structure.

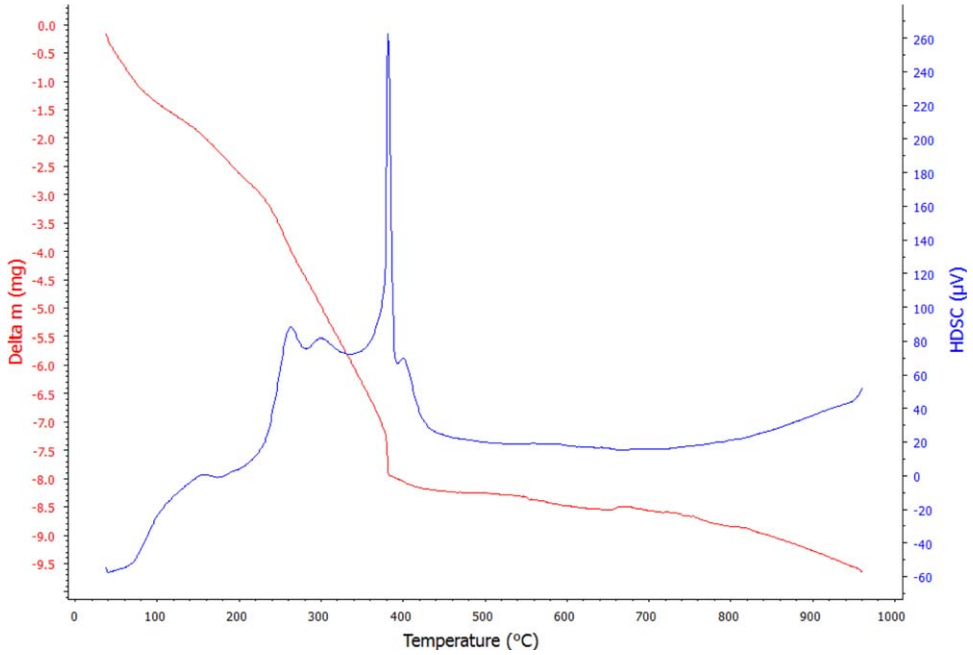

FIGURE 2. Differential scanning calorimetry and thermogravimetric (DSC-TGA) analysis of copper containing 45S5 nanofibers.

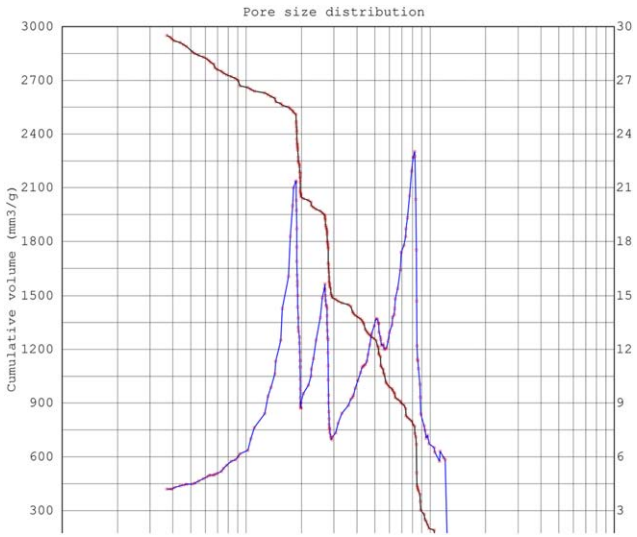

FIGURE 3. Mercury porosimetry of the composite gelatin/collagen/45S5+Cu scaffold.

Mercury porosimetery

Thermo Finnigan mercury intrusion porosimeter (PASCAL 140) was used for porosimetery analysis of nanocomposite scaffold. Pore distribution and total porosity were investigated with mercury porosimetery method. As shown in Figure 3, results demonstrated that the distribution of the pores was in the range of 10–200 μm for this nanocomposite scaffold. The measured porosity was around 80%. The average pore size was around 82 ± 22 μm.

XRD analysis: Crystallographic properties of nanofibrillar bioglass precipitated within the nanocomposite scaffold

Bioglass nanofibers were analyzed using XRD. Figure 4 shows diffractograms obtained from XRD for the nanofibrilar bioglass. The diffractograms have weak peaks representing a type of amorphous or semicrystalline nature. These peaks can be ascribed to combeite and silicorhenanite according to the ICCD database.

FTIR analysis

FTIR analysis was performed to study the chemical characteristics of prepared nanocomposite scaffold. FTIR analysis also shows peaks related to chemical bonds formed by the combination of nanofibrilar bioglass with hydrogel and followed cross-linking with Genipin in the structure of nanocomposite scaffold. Figure 5 shows the FTIR spectra, in the 400–4000/cm spectral range, for nanocomposite containing heat-treated 45S5 bioglass nanofiber containing Cu ion before and after cross-linking with genipin. FTIR spectra of these samples exhibited two series of characteristic spectral bands such as: C=O stretch at 1662.1/cm for amide I, N–H bend and C–H stretch at 1546/cm for amide II, C–N stretch plus N–H in phase bending at 1244/cm for amide III, N–H stretching vibration at 3298/cm for the amide, which are the distinguishing features of gelatin and collagen.[39] In cross-linked hydrogel, we see similar peaks with a little shift as it has been previously reported.[39] In addition, three infrared bands are located at 464, 940, and 1084/cm, which are related to the silicate network and are attributed to the Si–O–Si bending vibration, Si–O stretching vibration, and asymmetric stretching vibration of Si–O–Si, respectively.[37,38,40] Interestingly, the peak located at about 1334/cm indicates formation of the chemical bond between carboxyl groups of hydrogel and Ca^{2+} ions of nanofibrilar bio glass. Same result has also been mentioned in former studies for gelatin and hydroxyapatite.[41,42]

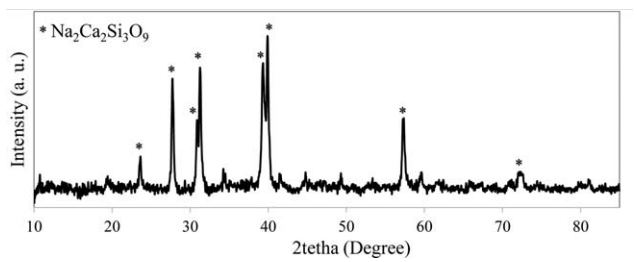

FIGURE 4. XRD patterns of sol-derived copper containing 45S5 BG nanofibers after heating at 700 °C.

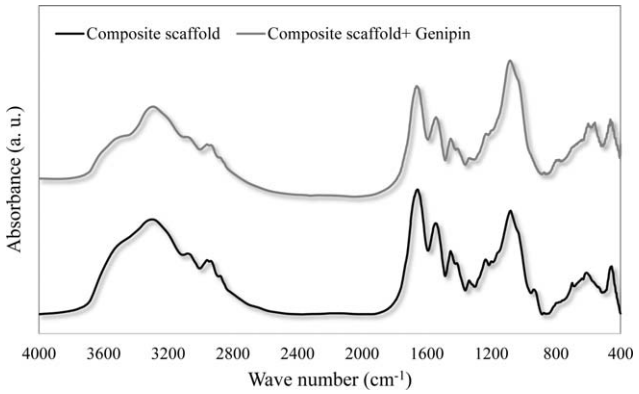

FIGURE 5. FTIR spectrum of composite scaffolds before and after crosslinking with genipin.

Morphological characterization of scaffold and cell attachment on the nanocomposite scaffold by SEM

SEM was used for observing morphology of nanofibers and porous structure of nanocomposite scaffold, also for studying the cells attachment on the nanocomposite scaffold. As shown in Figure 6, before heating at 700°C, the diameter of fibers were between 150 and 45 nm. After heating, the approximate diameter of these nanofibers were 200–450 nm. Obtained glass nanofibers represented coarse unsmooth morphology on the surface and showed fusion to each other after thermal treatment. Kim et al. succeed to fabricate bioglass nanofibers by electrospinning and they also accessed the response of osteoblasts on this nanocomposite scaffold.[19] Rboccacini et al. investigated the potential of bioactive scaffolds synthesized by bio glasses for bone tissue engineering.[2,21] Interconnected porous structure of nanocomposite scaffold is shown in Figure 7(a), diameters of the pores were in the range of 70–250, which is optimal for osteoblast adhesion and growth. SEM

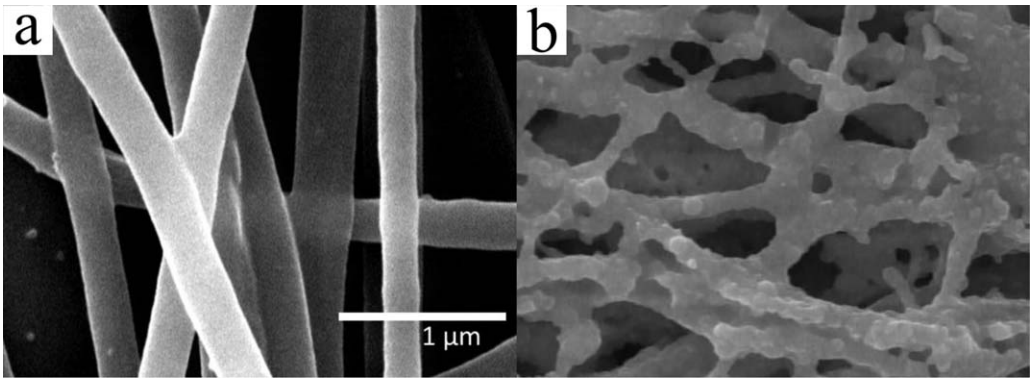

FIGURE 6. Scanning electron microscopy (SEM) micrograph of: a. nanofibers before heating, b. the nanofibers after heating at 700 °C.

pictures of differentiated osteoblast cells were obtained after culturing the cells on the prepared scaffolds. As shown in Figure 7(b), the cells have penetrated into nanocomposite scaffold pores, cell adhesions can be seen, and the cells have completely attached and expanded on the surface of the scaffolds. This biomimetic nanocomposite scaffold, mimicked ECM and provided an environments suitable for the osteoblast cells adherence and growth.

Cell viability and proliferation assay by MTT

MTT assay was performed at days 1, 2, and 4, on nanocomposite scaffolds including nanofibrilar sol-gel derived 45S5 bioglass containing copper. As shown by MTT assay (Figure 8), this scaffold did not have any negative effects on the proliferation rate of differentiated osteoblasts compared to two-dimensional culture on the surfaces of tissue cell culture. No significant differences were observed between nanocomposite scaffolds containing copper nanofibrilar 45S5 bioglass and the control group in all mentioned times, which indicates that this nanocomposite scaffold had no toxic effects on viability of the cells.

Gene expression analysis by qRT-PCR

After 21 days osteogenic induction, mRNA level expression of osteoblast markers was investigated by qRT-PCR (Figure 9). As shown in this figure, after the incubation time, osteoblasts differentiated from hEnSCs, on the Nano composite scaffold (three-dimensional culture) expressed higher phenotypic markers like osteonectin, osteopontin and ALP compared to the tissue culture plate group (two-dimensional culture).

ALP activity results

ALP activity is shown in Figure 10, there was higher volume of ALP production in the nanocomposite scaffold and two-dimensional culture in all days compared to control group.

DISCUSSION

Recently, various nanocomposite scaffolds with different shapes, e.g., fibrous membrane and three-dimensional porous scaffolds composed of bioactive glasses (nanoparticles and nanofibers) and polymeric materials (natural and synthetic) has been fabricated. Kim et al. for the first time produced nanocomposite scaffold containing PLA and bioglass nanofibers with sol-gel method combined with electrospinning. Osteoblastic activity was investigated on these nanocomposite scaffolds and results indicated improved osteoblastic activity by increasing the bioglass nanofibers.[43] Kim et al. also investigated the attachment of human osteoblast like cells on the nanocomposite scaffolds containing bioglass nanofibers and collagen.[11] Lee et al. fabricated nanocomposite scaffolds containing bioglass nanofibers and PCL, and studied growth of the osteoblast cells (MC3T3-

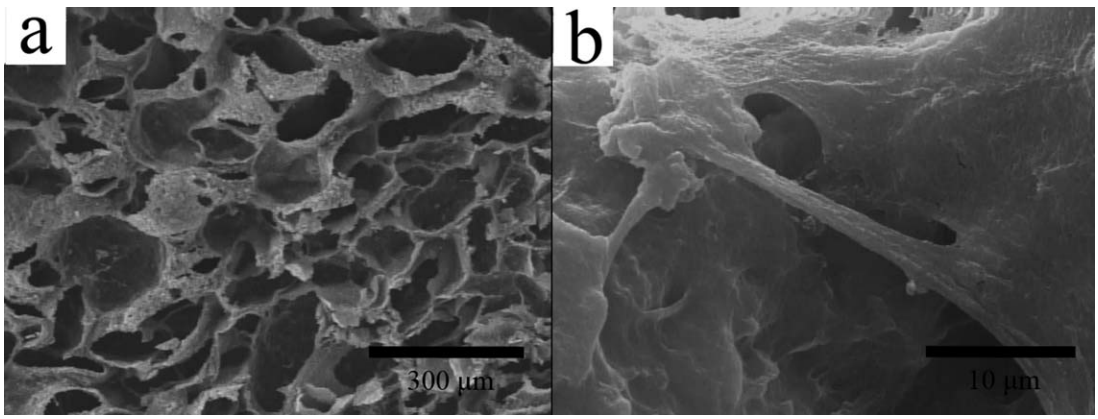

FIGURE 7. Scanning electron microscopy (SEM) micrograph of: a. the composite gelatin/collagen/45S5 bioglass nanofibers containing Cu, b. cultured cells on composite scaffold.

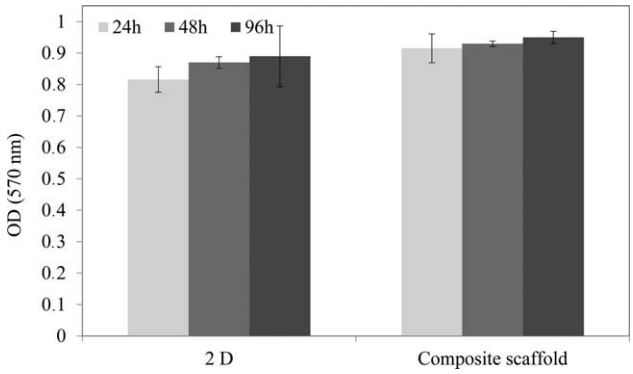

FIGURE 8. Determination of cell viability with the MTT assay. MTT assay was used as a measure of the survival of cells seeded into scaffolds in 3D and 2D at 24, 48 and 96 hrs of culture. Data are expressed as mean ± SD of three independent experiments in duplicate.

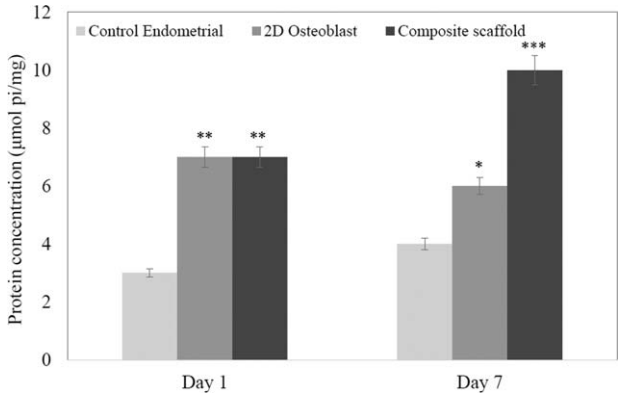

FIGURE 10. Alkaline phosphatase production of cells in day1 and day7 after cell seeding.

E1).[44] In this study, we fabricate a new nanocomposite scaffold with modifications in structure of other nanocomposite scaffolds. The combination of electrospinning and sol–gel method was used to fabricate the copper doped 45S5 bioglass nanofibers. The diameter of nanofibers was similar to previous studies, but the protocol was modified and PVA was used instead of PVB and PCL, and copper ion was incorporated in the bioglass network instead of Ca^{2+}. DSC analysis was used to get right heat treatment for stabilizing the bioglass nanofibers and elimination of nitrate component from bioglass network. Nychka et al. reported the best temperature for stabilizing the bioglass network and elimination of all organic component was 700°C.[38,45] DSC showed similar results for copper doped 45S5 bioglass nanofibers and before 700°C all nitrate and organic component were eliminated and bioglass network was stabilized. FTIR analysis was performed prior and after stabilizing of nanofibers at 700°C. Results showed that all nitrate and organic components were eliminated after stabilizing the nanofibers and chemical bonds related to bioglass structure[19,38] were revealed after heat treatment of nanofibers. Observed peaks in XRD spectrum were related to formation of combeite according to International Centre for Diffraction Data (ICCD) database. Characterized peaks are composed of

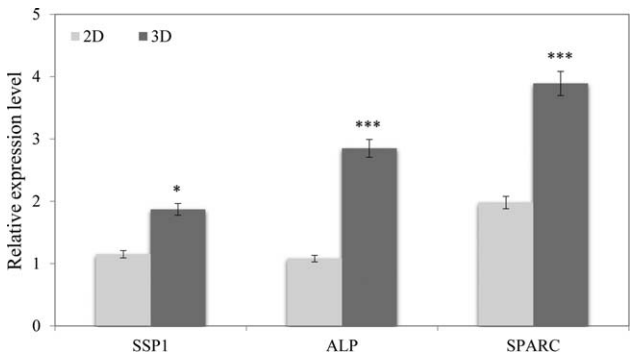

FIGURE 9. Quantitative mRNA expression analysis of osteoblast-like cells derived from human EnSCs seeded on scaffolds after 21 days. The result of mRNA expression on tissue culture plate (2D) and scaffolds (3D) compared to undifferentiated hEnSCs. (n = 3 biological samples, mean ± SD).

two sodium calcium silicate phases, including silicorhenanite (Na_2Ca_4 $(PO_4)_2SiO_4$) and combeite ($Na_2Ca_2Si_3O_9$).[23,46] It was mentioned that the silicorhenanite phases that were founded in this analysis are isostructural to apatite. Addition of Cu into the bioglass structure did not affect the formation of sodium calcium silicate phases, which has been reported in the literature.[22] These peaks showed the semicrystalline and amorphous properties of nanofibers. According to Chen et al.[46] studies, this phase is favorable for bioglass because it increases the strength of scaffold, and also when scaffold is implanted in the body, combiete transforms to biodegradable and bioactive calcium phosphate. Addition of copper to the structure of bioglass nanofibers does not affect the formation of Na–Ca–Si phase, which is similar to a previous study.[22] After confirming the bioglass structure, nanofibers were mixed with collagen and gelatin for the fabrication of porous nanocomposite scaffolds by using freeze-drying method. Genipin was used as a specific cross-linker of collagen and gelatin.[47,48] Mercury porosimetery was used to measure the pores' diameter and porosity of nanocomposite scaffold. The average of pores' diameter was 82 ∓ 22, and the total porosity was between 70% and 80%. According to the size of osteoblasts (∼20 μm) and the length of MSCs,[49] it seems that the pore size and distribution of porosity in this nanocomposite scaffold were enough for MSCs and osteoblast immigration and penetration and growth through the scaffold. Pores' distribution in this nanocomposite scaffold is suitable for osteoblast growth and migration according to Murphy and O'Brien[50] studies. The surface and morphology of scaffold were investigated with SEM. Porous structure was observed in SEM photomicrographs, and the diameter of pores were between 70 and 250 μm, which confirms the mercury porosimetery results according to previous studies; porosity of this nanocomposite scaffold is suitable for osteoblast growth.[50,51] Cytotoxicity of scaffold was examined with MTT assay, and the results showed that the prepared scaffold is nontoxic. After isolation and culture of the hEnSCs, dexamethasone, glyserophosphate, and ascorbic acid were used as differentiating medium. After 21 days, alizarin red staining was used as mineralization index. Enzyme assay (ALP) and osteoblast

gene (osteonectin, osteopointin, and alkaline phosphatase) assay were used for studying the osteoblast activity. Alkaline phosphatase enzyme activity was studied as mineralization index of osteoblast-like cells at days 1 and 7. ALP assay showed an increased activity of ALP in day 7 rather than two-dimensional culture. Higher volume production of ALP was observed in nanocomposite scaffolds and two-dimensional cultures compared to the control group (in all days). Results of gene assay studies showed expression of osteoblast genes, confirming the enzymatic assay. The result shows that three-dimensional culture of cells can provide suitable condition for cell survival and more differentiation especially in this study that 3D culture was done on copper-doped nanocomposite scaffold. Cell attachment was investigated with SEM. Osteoblast-like cells were attached and infiltrated to the porous nanocomposite scaffold. According to the obtained results, this nanocomposite scaffold is a suitable and nontoxic surface for attachment and adherence of osteoblast-like cells.

CONCLUSION

In this study, nanocomposite scaffold containing gelatin–collagen- and copper-doped nanofibrilar 45S5 bioglass was fabricated. Nanofibrilar bioglass (prepared with sol–gel method) was fabricated by electrospinning process, and the nanofibers were then mixed with hydrogel matrix containing gelatin and collagen. Structural analysis confirmed the formation of desirable phases of bioglass nanofiber. The growth and viability of differentiated osteoblast cells were investigated on this biomimetic scaffold mimicking the natural bone structure. Cellular biocompatibility and enzymatic and gene assays illustrated that scaffolds containing copper ion within the bioglass structure had more viability and osteoblast growth in comparison with two-dimensional culture. Copper ion increased the growth of osteoblasts on nanocomposite scaffold containing nanofibrous bioglass. Thus, the results obtained from this study indicated that the prepared scaffold, potentially, is an appropriate scaffold for bone tissue engineering.

REFERENCES

1. Langer R, Vacanti JP. Tissue engineering. Science 1993; 260: 920–926 [cited 11 November 2014]. Available from: http://www.ncbi.nlm.nih.gov/pubmed/8493529
2. Boccaccini AR, Blaker JJ. Bioactive composite materials for tissue engineering scaffolds. Expert Rev Med Devices 2005;2:303–317 [cited 5 April 2014]. Available from: http://www.ncbi.nlm.nih.gov/pubmed/16288594
3. Puska M, Aho AJ, Vallittu P. Polymer composites for bone reconstruction. Advances in Composite Materials - Analysis of Natural and Man-Made Materials, Dr. Pavla Tesinova (Ed.), ISBN: 978-953-307-449-8, InTech, 2011, Chapter 3, 55-72. Available from: http://www.intechopen.com/books/advances-incomposite-materials-analysis-of-natural-and-man-made-materials/polymer-composites-for-bone-reconstruction.
4. Teo W, Inai R, Ramakrishna S. Technological advances in electrospinning of nanofibers. Sci Technol Adv Mater. 2011;12:013002. Available from: http://stacks.iop.org/14686996/12/i=1/a=013002?key=crossref.a23c34c656dbebad703536d8a659fe57
5. Li M, Mondrinos MJ, Gandhi MR, Ko FK, Weiss AS, Lelkes PI. Electrospun protein fibers as matrices for tissue engineering. Biomaterials 2005;26:5999–6008.
6. Sell SA, Wolfe PS, Garg K, McCool JM, Rodriguez IA, Bowlin GL. The Use of Natural Polymers in Tissue Engineering: A Focus on Electrospun Extracellular Matrix Analogues. Polymers. 2010;2:522–53. Available from: http://www.mdpi.com/2073-4360/2/4/522/
7. Kamalian R, Yazdanpanah A, Moztarzadeh F, Ravarian R, Moztarzadeh Z, Tahmasbi M, Mozafari M. Synthesis and characterization of bioactive glass/forsterite nanocomposites for bone and dental implants. Ceramics Silikaty, 2012,56(4):331–340.
8. Cormack AN, Tilocca A. Structure and biological activity of glasses and ceramics. Philos Trans R Soc A Math Phys Eng Sci. 2012;370:1271–80. Available from: http://discovery.ucl.ac.uk/1340479/
9. Vallet-Regi M, Izquierdo-Barba I, Colilla M. Structure and functionalization of mesoporous bioceramics for bone tissue regeneration and local drug delivery. Philos Trans R Soc A: Math Phys Eng Sci 2012;370:1400–1421.
10. Oryan A, Alidadi S, Moshiri A, Maffulli N. Bone regenerative medicine: Classic options, novel strategies, and future directions. J Orthop Surg Res 2014;9:1–27.
11. Kim H-W, Song J-H, Kim H-E. Bioactive glass nanofiber-collagen nanocomposite as a novel bone regeneration matrix. J Biomed Mater Res A 2006;79:698–705 [cited 25 August 2014]. Available from: http://www.ncbi.nlm.nih.gov/pubmed/16850456
12. Mozafari M, Rabiee M, Azami M, Maleknia S. Biomimetic formation of apatite on the surface of porous gelatin/bioactive glass nanocomposite scaffolds. Appl Surf Sci 2010;257:1740–1749 [cited 15 February 2015]. Available from: http://linkinghub.elsevier.com/retrieve/pii/S0169433210012262
13. Moosavifar MJ, Moztarzadeh F, Azami M. Preparation of Mineralized Electrospun Fibers as a Biomimetic Nanocomposite. Int J Polym Mater Polym Biomater [Internet]. 2014;63:576–82. Available from: http://www.tandfonline.com/doi/abs/10.1080/00914037.2013.854229
14. Olszta MJ, Cheng X, Jee SS, Kumar R, Kim YY, Kaufman MJ, Douglas EP, Gower LB. Bone structure and formation: A new perspective. Mater Sci Eng R: Reports 2007;58:77–116.
15. Zheng W, Zhang W, Jiang X. Biomimetic collagen nanofibrous materials for bone tissue engineering. Adv Eng Mater B 2010;12: 451–466 [cited 7 August 2014]. Available from: http://doi.wiley.com/10.1002/adem.200980087
16. Lee HH, Yu HS, Jang JH, Kim HW. Bioactivity improvement of poly(ϵ-caprolactone) membrane with the addition of nanofibrous bioactive glass. Acta Biomater 2008;4:622–629 [cited 27 July 2014]. Available from: http://www.ncbi.nlm.nih.gov/pubmed/18171636
17. Shin S-H, Purevdorj O, Castano O, Planell JA, Kim H-W. A short review: Recent advances in electrospinning for bone tissue regeneration. J Tissue Eng. 2012;3. Available from: http://tej.sagepub.com/lookup/doi/10.1177/2041731412443530
18. Kanani AG, Bahrami SH. Review on Electrospun Nanofibers Scaffold and Biomedical Applications. Trends Biomater Artif Organs. 2010;24:93–115.
19. Kim H-W, Kim H-E, Knowles JC. Production and potential of bioactive glass nanofibers as a next-generation biomaterial. Adv Funct Mater 2006;16:1529–1535 [cited 25 August 2014]. Available from: http://doi.wiley.com/10.1002/adfm.200500750
20. Mačkovič M, Hoppe A, Detsch R, Mohn D, Stark WJ, Spiecker E, Boccaccini AR. Bioactive glass (type 45S5) nanoparticles: in vitro reactivity on nanoscale and biocompatibility. J Nanoparticle Res. 2012;14:966–987. Available from: http://link.springer.com/10.1007/s11051-012-0966-6
21. Boccaccini AR, Erol M, Stark WJ, Mohn D, Hong Z, Mano JF. Polymer/bioactive glass nanocomposites for biomedical applications: A review. Compos Sci Technol 2010;70:1764–1776 [cited 20 November 2014]. Available from: http://linkinghub.elsevier.com/retrieve/pii/S0266353810002289
22. Hoppe A, Meszaros R, Stähli C, Romeis S, Schmidt J, Peukert W, Marelli B, Nazhat SN, Wondraczek L, Lao J, Jallot E, Boccaccini AR. In vitro reactivity of Cu doped 45S5 Bioglass® derived scaffolds for bone tissue engineering. J Mater Chem B. 2013;1:5659–74.
23. Bretcanu O, Chatzistavrou X, Paraskevopoulos K, Conradt R, Thompson I, Boccaccini AR. Sintering and crystallisation of 45S5 Bioglass® powder. J Eur Ceram Soc. 2009;29:3299–306. Available from: http://linkinghub.elsevier.com/retrieve/pii/S0955221909003525

24. Yu B, Turdean-Ionescu CA, Martin RA, Newport RJ, Hanna JV, Smith ME, Jones JR. Effect of Calcium Source on Structure and Properties of Sol–Gel Derived Bioactive Glasses. Langmuir. 2012; 28:17465–76. Available from: http://pubs.acs.org/doi/abs/10.1021/la303768b
25. Mourino V, Cattalini JP, Boccaccini AR. Metallic ions as therapeutic agents in tissue engineering scaffolds: an overview of their biological applications and strategies for new developments. J R Soc Interface. 2012;9:401–19. Available from: http://rsif.royalsocietypublishing.org/cgi/doi/10.1098/rsif.2011.0611
26. Schieker M, Seitz H, Drosse I, Seitz S, Mutschler W. Biomaterials as Scaffold for Bone Tissue Engineering. Eur J Trauma. 2006;32: 114–24. Available from: http://link.springer.com/10.1007/s00068-006-6047-8
27. Singh RK, Gaikwad SM, Chatterjee S, Ray P. Stem Cells: The Holy Grail of Regenerative Medicine. In: Cai W editor. Eng Transl Med. London: Springer London; 2014. Chapter 2, 19-69. Available from: http://link.springer.com/10.1007/978-1-4471-4372-7_2
28. Bagher Z, Azami M, Ebrahimi-Barough S, Mirzadeh H, Solouk A, Soleimani M, Ai J, Nourani MR, Joghataei MT. Differentiation of Wharton's Jelly-Derived Mesenchymal Stem Cells into Motor Neuron-Like Cells on Three-Dimensional Collagen-Grafted Nanofibers. Mol Neurobiol. 2016;53:2397–408. Available from: http://link.springer.com/10.1007/s12035-015-9199-x
29. Pittenger MF, Mackay a. M, Beck SC, Jaiswal RK, Douglas R, Mosca JD, Moorman MA, Simonetti DW, Craig S, Marshak DR. Multilineage potential of adult human mesenchymal stem cells. Science 1999;284:143–147.
30. Bobis S, Jarocha D, Majka M. Mesenchymal stem cells: Characteristics and clinical applications. Folia Histochem Cytobiol 2006;44: 215–230.
31. Gargett CE, Masuda H. Adult stem cells in the endometrium. Mol Hum Reprod 2010;16:818–834.
32. Gargett CE, Schwab KE, Zillwood RM, Nguyen HPT, Wu D. Isolation and culture of epithelial progenitors and mesenchymal stem cells from human endometrium. Biol Reprod 2009;80:1136–1145.
33. Schwab KE, Chan RWS, Gargett CE. Putative stem cell activity of human endometrial epithelial and stromal cells during the menstrual cycle. Fertil Steril. 2005;84:1124–30. Available from: http://linkinghub.elsevier.com/retrieve/pii/S0015028205014214
34. Azami M, Ai J, Ebrahimi-Barough S, Farokhi M, Fard SE. In vitro evaluation of biomimetic nanocomposite scaffold using endometrial stem cell derived osteoblast-like cells. Tissue Cell 2013;45:328–337.
35. Shamosi A, Mehrabani D, Azami M, Ebrahimi-Barough S, Siavashi V, Ghanbari H, Sharifi E, Roozafzoon R, Ai J. Differentiation of human endometrial stem cells into endothelial-like cells on gelatin/chitosan/bioglass nanofibrous scaffolds. Artif Cells, Nanomedicine, Biotechnol. 2016; Feb 16: 1–11. Available from: http://www.tandfonline.com/doi/full/10.3109/21691401.2016.1138493
36. Ebrahimi-Barough S, Kouchesfahani HM, Ai J, Massumi M. Differentiation of human endometrial stromal cells into oligodendrocyte progenitor cells (OPCs). J Mol Neurosci 2013;51:265–273. Available from: http://www.ncbi.nlm.nih.gov/pubmed/23338937
37. Cacciotti I, Lombardi M, Bianco A, Ravaglioli A, Montanaro L. Sol–gel derived 45S5 bioglass: synthesis, microstructural evolution and thermal behaviour. J Mater Sci Mater Med. 2012;23: 1849–66. Available from: http://link.springer.com/10.1007/s10856-012-4667-6
38. Pirayesh H, Nychka JA. Sol-Gel Synthesis of Bioactive Glass-Ceramic 45S5 and its in vitro Dissolution and Mineralization Behavior. Bose S editor. J Am Ceram Soc. 2013;96:1643–50. Available from: http://doi.wiley.com/10.1111/jace.12190
39. Nguyen T, Lee B. Fabrication and characterization of cross-linked gelatin electro-spun nano-fibers. J Biomed Sci Eng. 2010;03:1117–24. Available from: http://www.scirp.org/journal/PaperDownload.aspx?DOI=10.4236/jbise.2010.312145
40. Srivastava AK, Pyare R. Characterization of CuO substituted 45S5 bioactive glasses and glass—Ceramics. Int J Sci Technol Res 2012;1:28–41.
41. Kikuchi M, Itoh S, Ichinose S, Shinomiya K, Tanaka J. Self-organization mechanism in a bone-like hydroxyapatite/collagen nanocomposite synthesized in vitro and its biological reaction in vivo. Biomaterials. 2001;22:1705–11. Available from: http://linkinghub.elsevier.com/retrieve/pii/S0142961200003057
42. Chang MC, Tanaka J. FT-IR study for hydroxyapatite/collagen nanocomposite cross-linked by glutaraldehyde. Biomaterials 2002;23:4811–4818. Available from: http://linkinghub.elsevier.com/retrieve/pii/S0142961202002326
43. Ferreira AM, Gentile P, Chiono V, Ciardelli G. Collagen for bone tissue regeneration. Acta Biomater 2012;8:3191–3200.. Available from: http://linkinghub.elsevier.com/retrieve/pii/S1742706112002620
44. Jo J-H, Lee E-J, Shin D-S, Kim H-EH-W, Koh Y-H, Jang J-H. In vitro/in vivo biocompatibility and mechanical properties of bioactive glass nanofiber and poly(epsilon-caprolactone) composite materials. J Biomed Mater Res B: Appl Biomater 2009;91:213–220 [cited 5 August 2014]. Available from: http://www.ncbi.nlm.nih.gov/pubmed/19422050.
45. Bahniuk MS, Pirayesh H, Singh HD, Nychka JA, Unsworth LD. Bioactive Glass 45S5 Powders: Effect of Synthesis Route and Resultant Surface Chemistry and Crystallinity on Protein Adsorption from Human Plasma. Biointerphases. 2012;7:1–15. Available from: http://scitation.aip.org/content/avs/journal/bip/7/1/10.1007/s13758-012-0041-y
46. Chen QZ, Thompson ID, Boccaccini AR. 45S5 Bioglass®-derived glass–ceramic scaffolds for bone tissue engineering. Biomaterials 2006;27:2414–2425. Available from: http://linkinghub.elsevier.com/retrieve/pii/S0142961205010422
47. Li W, Wang H, Ding Y, Scheithauer EC, Goudouri O-M, Grünewald A, Detsch R, Agarwal S, Boccaccini AR. Antibacterial 45S5 Bioglass®-based scaffolds reinforced with genipin cross-linked gelatin for bone tissue engineering. J Mater Chem B. 2015; 3:3367–78. Available from: http://xlink.rsc.org/?DOI=C5TB00044K
48. Bigi a, Cojazzi G, Panzavolta S, Roveri N, Rubini K. Stabilization of gelatin films by crosslinking with genipin. Biomaterials 2002; 23:4827–4832. Available from: http://www.ncbi.nlm.nih.gov/pubmed/12361622
49. Ge J, Guo L, Wang S, Zhang Y, Cai T, Zhao RCH, Wu Y. The size of mesenchymal stem cells is a significant cause of vascular obstructions and stroke. Stem Cell Rev Reports 2014;10:295–303.
50. Murphy CM, O'Brien FJ. Understanding the effect of mean pore size on cell activity in collagen-glycosaminoglycan scaffolds. Cell Adhes Migr 2010;4:377–381.
51. Haugh MG, Murphy CM, O'Brien FJ. Novel freeze-drying methods to produce a range of collagen-glycosaminoglycan scaffolds with tailored mean pore sizes. Tissue Eng Part C: Methods 2010;16:887–894.